Acta Oceanol. Sin., 2025, Vol. 44, No. 4, P. 1–19
https://doi.org/10.1007/s13131-025-2465-5

Paleoceanographic and paleoenvironmental changes in the high-latitude Southern Ocean during late Quaternary: progress and prospects based on the Chinese Antarctic Expeditions

Li Wu[1, 2, 3, 4, 5], Rujian Wang[2*], Wenshen Xiao[2], Qingmiao Li[2], Kaitao Ni[1], Ran Xu[1], Yi Chen[1]

[1] Laboratory for Coastal Ocean Variation and Disaster Prediction, College of Ocean and Meteorology, Guangdong Ocean University, Zhanjiang 524088, China

[2] State Key Laboratory of Marine Geology, Tongji University, Shanghai 200092, China

[3] Key Laboratory of Climate, Resources and Environment in Continental Shelf Sea and Deep Sea of Department of Education of Guangdong Province, Guangdong Ocean University, Zhanjiang 524088, China

[4] Key Laboratory of Space Ocean Remote Sensing and Application, Ministry of Natural Resources, Beijing 100081, China

[5] Key Laboratory for Polar Geology and Marine Mineral Resources of Ministry of Education, China University of Geosciences (Beijing), Beijing 100083, China

Received 29 August 2024; accepted 25 October 2024

© Chinese Society for Oceanography and Springer-Verlag GmbH Germany, part of Springer Nature 2025

Abstract

This review compiles studies on paleoceanographic and paleoenvironmental changes in the high-latitude Southern Ocean during the late Quaternary based on Chinese Antarctic Expeditions. Four major findings are summarized as follows. (1) Diatom compositions in sediment record sea surface condition changes in the Bransfield Strait and Cosmonaut Sea, indicating an increase in sea ice cover since the Mid-Holocene for both areas, possibly linked to cold water mass injection from the Weddell Sea ice shelf. (2) Export productivity records from Antarctic marginal seas show a glacial-interglacial variation pattern, with higher and lower productivity during the interglacial and glacial periods, respectively, controlled by both the intensity of Circumpolar Deep Water upwelling and sea ice cover. An overall increase of export productivity from Marine Isotope Stage (MIS) 12 to MIS 6 is noticed. (3) Ventilation state of the abyssal Southern Ocean is closely related to global climate change and atmospheric CO_2 concentrations, with elevated ventilation efficiency during deglacial periods responsible for elevated atmospheric CO_2 concentrations. (4) Antarctic marine-based ice sheets/glaciers wax and wane in line with global and regional ice volume changes, predominantly subject to oceanic forcing, while land-based ice sheets might only reorganize in specific glacial intervals. Despite significant progress in understanding the role of the Southern Ocean and the Antarctic Ice Sheet within the global climate system, challenges remain in sample collection and research methods. Future studies should aim to collect samples from a broader range of latitudes, ensure higher quality and longer temporal span, resolve dating issues, reconstruct seawater temperature, and focus on reconstructions of Southern Ocean carbon cycling and changes of intermediate to deep water masses.

Key words Southern Ocean, Antarctica, Chinese Antarctic Expedition (CHINARE), paleoceanography and paleoclimate, Pleistocene

Citation Wu Li, Wang Rujian, Xiao Wenshen, Li Qingmiao, Ni Kaitao, Xu Ran, Chen Yi. 2025. Paleoceanographic and paleoenvironmental changes in the high-latitude Southern Ocean during late Quaternary: progress and prospects based on the Chinese Antarctic Expeditions. Acta Oceanologica Sinica, 44(4): 1–19, doi: 10.1007/s13131-025-2465-5

Foundation item: The National Natural Science Foundation of China under contract Nos 42030401 and 42276077; the Open Foundation of State Key Laboratory of Marine Geology, Tongji University under contract No. MGK202207; the Open Foundation Project of the Key Laboratory of Polar Geology and Marine Mineral Resources of Ministry of Education, China University of Geosciences (Beijing), under contract Nos PGMR-2024-102 and PGMR-2023-304; the Start-up Foundation of Guangdong Ocean University under contract No. 060302032110.

*Corresponding author, E-mail: rjwang@tongji.edu.cn

http://www.aosocean.com
E-mail: ocean2@hyxb.org.cn

1 Introduction

Antarctic Ice Sheet (AIS) and the Southern Ocean represent the two most significant geographical units in the high latitudes of the Southern Hemisphere. The AIS, covering over 98% of the Antarctic continent, holds the largest ice mass on modern Earth, it spans nearly 14×10^6 km^2 and contains 26.5×10^6 km^3 of ice, which is equivalent to approximately 58 m of potential sea-level rise (Fretwell et al., 2013). And thus, even partial melting of the AIS would induce significant global mean sea level rise (Blackburn et al., 2020; DeConto and Pollard, 2016). The Southern Ocean acts as a vital conduit connecting global oceans, facilitating the transfer of heat, gases, nutrients, and water masses (Bostock et al., 2013). In particular, it acts as an important interface of CO_2 exchange between the ocean and the atmosphere because it represents the major upwelling branch of the Global Thermohaline Overturning Circulation (Anderson et al., 2009; Jaccard et al., 2013; Marshall and Speer, 2012; Sigman et al., 2010).

Scientific investigation in this region primarily focuses on two key issues. (1) How does the AIS influence and respond to regional and global climate changes over varying timescales (e.g., Cook et al., 2013; Passchier, 2011; Patterson et al., 2014; Ge et al., 2022; Wilson et al., 2018; Wu et al., 2018; An et al., 2024)? (2) What role does the Southern Ocean play in regulating atmospheric CO_2 levels (e.g., Anderson et al., 2009, 2014a; Jaccard et al., 2016; Martínez-Garcia et al., 2011; Meckler et al., 2013; Wu et al., 2017, 2018)? Marine sediment cores from the high latitudes of the Southern Ocean are crucial archives to address these questions. In recent decades, studies utilizing marine sediment cores have increasingly highlighted the significant role of the Southern Hemisphere's high latitudes in regulating global climate and environment (Sikes et al., 2023; Starr et al., 2021; An et al., 2024; Lamy et al., 2024). Notably, research based on Chinese Antarctic Expedition (CHINARE) has made substantial contributions, which were primarily focused on sea surface conditions, export productivity, abyssal ventilation of the Southern Ocean and dynamics of glaciers around AIS (e.g., Chen et al., 2024; Ge et al., 2022; Hu et al., 2023; Li et al., 2021, 2022; Liu et al., 2024; Nie et al., 2022; Tang et al., 2022; Wang et al., 2022b; Wu et al., 2017, 2018, 2019, 2020). China initiated Antarctic expeditions in 1984, marking four decades of exploration this year. This review aims to synthesize the major findings achieved based on sediment cores retrieved during CHINARE and outlines perspectives for future studies.

2 Environmental setting

AIS is divided by the Trans-Antarctic Mountains into the East AIS (EAIS) and the West AIS (WAIS). Although the WAIS accounts for only 12% of the total AIS (Fretwell et al., 2013), it is considered the most dynamic part of AIS due to its significant portion lying below sea level (DeConto and Pollard, 2016; Pollard and DeConto, 2009; Tigchelaar et al., 2018). In contrast, a large portion of the EAIS is situated on land and is generally considered to be less variable during the Quaternary (Passchier, 2011). However, about one-third of the EAIS is marine-based and has also been shown to be dynamic (Fretwell et al., 2013; Golledge et al., 2017; Wilson et al., 2018).

The Southern Ocean features a series of oceanic fronts defined by gradients in water mass characteristics such as salinity, temperature, and nutrient concentrations (Orsi et al., 1995). These fronts divide the Southern Ocean into distinct zones (Fig. 1; Orsi et al., 1995; Orsi and Whitworth Ⅲ, 2005). From south to north, these fronts include the Southern Antarctic Circumpolar Current Front (SACCF), the Southern Polar Front (SPF), the Subantarctic Front (SAF), and the Subtropical Front (STF; Orsi et al., 1995). The Antarctic zone lies south of the SPF, the polar frontal zone is between the SPF and SAF, and the subantarctic zone is located between the SAF and STF (Orsi et al., 1995).

Oceanic currents in the Southern Ocean primarily consist of the eastward-flowing Antarctic Circumpolar Current (ACC) and the westward-flowing Antarctic slope current/coastal current (Orsi et al., 1995). These currents are separated by clockwise-rotating mesoscale eddies, which form the Antarctic divergence zone and coincide with the southern boundary of the ACC, namely the SACCF. Additionally, clockwise gyres develop in bay areas such as Prydz Bay, the Ross Sea, and the Weddell Sea (Orsi et al., 1995).

Several major water masses exist in the Southern Ocean (Orsi et al., 1995). Antarctic Bottom Water (AABW), the densest water mass type, is found at the deepest part of the Southern Ocean. Above the AABW lies the Circumpolar Deep Water (CDW), which is the predominant water mass in the Southern Ocean. Antarctic Intermediate Water (AAIW) is produced at the SPF, and Subantarctic Mode Water (SAMW) is produced at the Subantarctic Zone. These water masses are formed through rapid sinking of Antarctic surface water.

Maximum sea ice cover occurs in the austral winter, reaching approximately 18.3×10^6 km² in September and forming a continuous ring around Antarctica (Comiso, 2010). In contrast, minimum sea ice cover is observed in the austral summer, around February, covering about 3×10^6 km² predominantly in the western Weddell Sea, Bellingshausen Sea, Amundsen Sea, and part of the Ross Sea and southern Indian Ocean (Comiso, 2010). During the Last Glacial Maximum (LGM), studies based on diatom assemblages and model simulations suggest that both summer and winter sea ice limits extended further north. The winter sea ice limit during the LGM likely reached the position of the modern SPF, while the summer sea ice limit generally expanded to approximately the

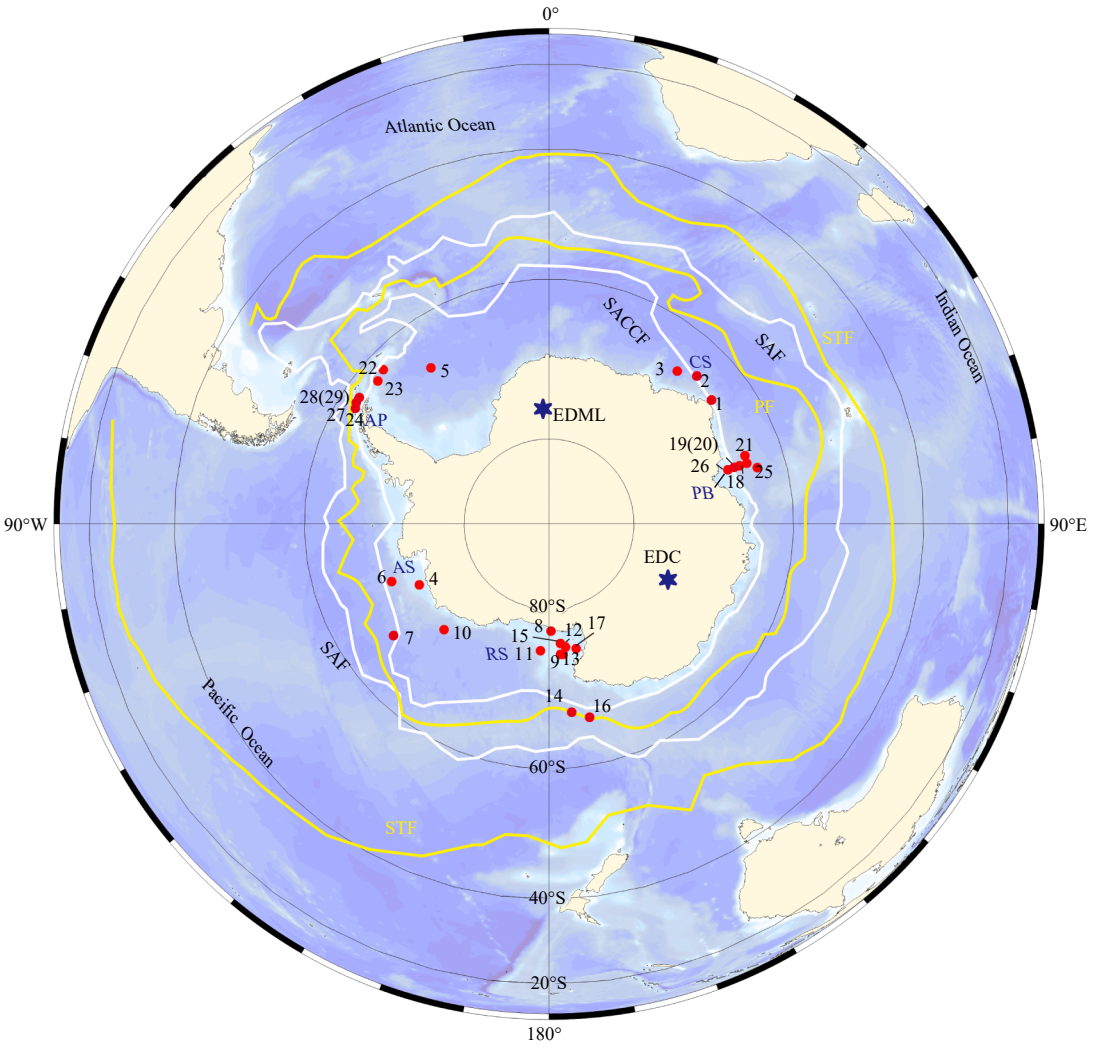


Fig. 1. Environmental setting of the Antarctic and Southern Ocean region and core sites compiled in this study. The numbered red dots represent the sediment cores collected during CHINARE (see Table 1). Ice core sites EPICA Dome C (EDC) and EPICA Dome Maud Land (EDML) (blue six-pointed stars) are from EPICA Community Members (2004). SACCF: Southern Antarctic Circumpolar Current Front. PF: Polar Front. SAF: Sub-Antarctic Front. STF: Sub-Tropical Front. Frontal system were according to Orsi et al. (1995) and Bostock et al. (2013). This figure is plotted in Ocean Data View (Schlitzer, 2009). PB: Pyrdz Bay. CS: Cosmonaut Sea. AP: Antarctic Peninsula. AS: Amundsen Sea. RS: Ross Sea.

modern winter sea ice edge (Crosta et al., 1998; Gersonde et al., 2005; Röthlisberger et al., 2010).

3 Data and proxies

3.1 *Sediment cores*

This review compiles data from marine sediment cores collected through CHINARE, focusing on five high-latitude regions in the Southern Ocean around Antarctica: Prydz Bay, Ross Sea, Amundsen Sea, the region around the Antarctic Peninsula, and Cosmonaut Sea (Fig. 1, Table 1). These sites are distributed across continental shelves, slopes, rises, and abyssal plains south to the polar front (62°S), with water depths ranging from 75 m to over 4 600 m. The cores were obtained using gravity corers and vary in length from 22 cm to 819 cm, spanning ages from several thousand years to 773 ka, and have average sedimentation rates ranging from <60 cm/ka. Sediment colors observed include greenish-gray, gray, yellowish-gray, and brownish-gray. The sediment mainly consists of clayey silt, silty clay, silty sand, sandy silt, and gravelly sand, with occasional dropstones.

Biogenic opal is the predominant biogenic component in the sediment, primarily consisting of diatoms, with minor amount of radiolarians and sponge spicules. The cores generally lack biogenic carbonates, though some layers contain planktonic foraminiferal species, mainly *Neogloboquadrina pachyderma* and a few endemic Antarctic benthic species such as *Miliammina arenacea*, *Trifarina earlandi*, and *Lagena* spp. (Fan et al., 2021). Table 1 lists a total of 29 published cores from CHINARE. The earliest core is PC10 from the 7th

Table 1. Information of sediment cores compiled in this study collected during CHINARE

Cruise	Number	Station	Latitude	Longitude	Depth/m	Core length/ cm	Age span/ ka	Reference
ANT37	1	C5/6-07	65°21′16″S	52°35′41″E	2 825	378	26	Hu et al. (2023) Chen et al. (2024)
ANT36	2	C4-05	64°41′27″S	44°56′16″E	3 871	22	6.5	Li et al. (2021)
	3	C3-09	65°58′48″S	39°57′36″E	4 368	29	17.3	Li et al. 2021
	4	A11-02	72°59′00″S	115°00′00″W	666	32	4.5	Lei et al. (2022)
ANT34	5	DC-11	66°24′39″S	37°04′52″W	2 162	422	34	Yang et al. (2021)
	6	A5-7	69°56′58″S	110°00′54″W	3 537	469	24.5	Zhang et al. (2023b)
	7	A2-10	67°02′10″S	125°35′31″W	4 217	454	773	Wang et al. (2022b) Tang et al. (2022)
	8	D5-12	62°25′31″S	39°01′48″W	2 556	456	105	Wang et al. (2023b)
ANT32	9	RBA08C	77°23′24″S	178°59′54″E	738	181	–	Xiu et al. (2017)
	10	RB16C	74°31′06″S	175°07′15″E	471	232	24.8	Liu et al. (2024); Song et al. (2022); Long et al. (2024)
	11	AMS01	72°18′14″S	135°02′42″W	3 812	373	325	Ju et al. (2019)
	12	RA05C	74°57′25″S	176°00′51″W	1878	280	–	Li et al. (2022)
ANT31	13	JB03	75°49′00″S	174°41′14″E	614	132	24.8	Liu et al. (2024)
	14	JB06	74°28′12″S	173°54′36″E	568	299	36.6	Huang et al. (2016); Fan et al. (2021)
	15	R22	67°13′12″S	173°09′00″E	2 906	412	512	Li et al. (2021)
	16	JB04	75°18′04″S	172°22′21″E	510.8	314	12.4	Zhao et al. (2017)
	17	R23	66°13′47″S	168°11′08″E	2 967	819	–	Chen et al. 2021
	18	R11	74°57′05″S	167°48′52″E	447.94	86	–	Xiu et al. (2017)
ANT30	19	P1-3	65°59′24″S	73°01′12″E	2 542	599	510	Liu et al. (2015)
	20	P1-2	65°00′36″S	72°56′24″E	2 860	624	523	Wu et al. (2017)
ANT29	21	P5-3	65°59′20″S	72°57′32″E	2 576	313	–	Wu et al., (2021)
	22	P4-1	64°55′12″S	70°41′24″E	3 162	421	495	Wu et al. (2017)
ANT28	23	D4-9	62°24′30″S	47°06′31″W	3 401	298	9.8	Yan et al. (2023)
	24	D3-7	62°52′33″S	50°10′46″W	3 429	319	35	Wang et al. (2014)
	25	D1-7	62°16′10″S	56°35′27″W	1 100	307	5.2	Nie et al. (2015)
ANT11	26	NP95-1	63°50′33″S	74°50′00″E	1 960	170	9.5	Gu et al., (1997)
ANT09	27	NP93-2	67°35′24″S	73°07′48″E	550	85	12.7	Hou et al. (1996)
	28	NG93-1	62°14′44″S	58°49′55″W	75	82	1.8	Gu et al. (1997)
ANT07	29	PC10	62°17′05″S	57°29′54″W	2 000	753	112.5	Wu and Lu (1998)

Note: – means no data.

CHINARE, while the most recent cores are C5/6-07 and C4-05 from the 37th CHINARE. The scarcity of published core data can be attributed to two main reasons: firstly, some expeditions, particularly the earlier ones, did not yield suitable sediment cores for study; secondly, establishing age-depth models for most CHINARE cores has proven challenging, which complicates further research.

3.2 *Age-depth model construction*

Establishing reliable age-depth models for sediment cores is fundamental to research in paleoenvironment, paleoceanography, and paleoclimate. For the cores collected during CHINARE, multiple techniques have been developed to address this need.

For sediment cores younger than 45 ka, AMS^{14}C dating of foraminiferal tests can provide accurate absolute ages by assuming a constant reservoir age (about 1 300 a) (Domack et al., 2001; Hajdas et al., 2021). However, due to poor preservation of biogenic carbonate in the Southern Ocean, this method is often limited (Tang et al., 2016, 2022; Wu et al., 2017; Xiao et al., 2016). As an alternative, dating the organic carbon of bulk sediments is used. Despite uncertainties related to old carbon contamination, which can affect the accuracy of the age of the bulk sediment organic fractions, a study from the Ross Sea suggests that old carbon contamination may remain constant for Holocene core sediments (Prothro et al., 2020). By subtracting this constant old carbon contamination, which is typically estimated using the core-top age, a reliable age-depth framework can be established. Consequently, most shorter sediment cores collected during CHINARE have been dated using this method (e.g., Chen et al., 2024; Hu et al., 2022, 2023; Li et al., 2021; Zhang et al., 2023a; Fan et al., 2021; Nie et al., 2014; Lei et al., 2022; Yan et al., 2023; Huang et al., 2016; Long et al., 2024).

Studies show a close coupling between productivity in the Southern Ocean and global and regional climate changes (Bonn et al., 1998). On glacial-interglacial timescales, higher export productivity was observed dur-

ing interglacials, and lower productivity was during glacials in the south of the SPF (Jaccard et al., 2013). This productivity-climate coupling relationship seems to persist even on millennial timescales (Lu et al., 2022), providing a reliable method for establishing age-depth models for longer sediment cores (Presti et al., 2011; Wu et al., 2017). Sediment cores such as P1-2, P1-3 (Tang et al., 2016; Wu et al., 2017), and A2-10 (Tang et al., 2022) have been dated using this approach.

In the open ocean regions around Antarctica, previous studies have demonstrated a strong correlation between the magnetic susceptibility records of sediment cores and Antarctic ice core dust records (Pugh et al., 2009; Weber et al., 2012; Xiao et al., 2016). On glacial-interglacial timescales, higher magnetic susceptibility during glacial periods corresponds to increased dust fluxes in Antarctic ice cores, while lower magnetic susceptibility during interglacial periods relates to decreased dust fluxes (Pugh et al., 2009). This coupling holds on millennial timescales, as supported by additional dating methods (Weber et al., 2012; Xiao et al., 2016), despite ongoing debates about the origin of sediment magnetization in the Southern Ocean (Xiao et al., 2016; Zhang et al., 2022). This approach offers a cost-effective, efficient, and high-resolution technique for establishing age-depth models of marine sediment cores retrieved from the Southern Ocean, such as Cores DC-11 and D5-12 (Yang et al., 2021; Wang et al., 2023b).

Near the Antarctic Peninsula, significant volcanic activities occurred during Late Quaternary (Ren, 1993). These volcanic activities resulted in deposition of tephra layers. Importantly, these tephra layers can be precisely dated using radiogenic isotopes. Consequently, chronological studies of these volcanic events have laid a solid foundation for correlating and dating volcanic ash layers in nearby sediment cores. As an illustration, tephra stratigraphy was successfully applied to date sediment Core D1-7, as reported by Nie et al. (2022).

3.3 *Proxy records*

3.3.1 *Surface seawater conditions*

Export productivity reflects sea surface conditions. In the Southern Ocean, common sedimentary proxies for export productivity include Total Organic Carbon (TOC) (Feng et al., 2023), biogenic opal (Tang et al., 2016), the Ba/Al count ratio and the Si/Al count ratio (Wu et al., 2017; Wang et al., 2022b), all of which are associated with diatoms. Export productivity records in marine sediments are controlled by sea surface productivity, but are potentially affected by preservation and burial efficiency at the sea floor (Jaccard et al., 2010). Lateral transport and winnowing by bottom currents controls their burial efficiency, while the preservation efficiency of these proxies varies significantly due to different controlling factors. For instance, TOC preservation is primarily linked to seawater dissolved oxygen content, and higher dissolved oxygen levels increase the chance of TOC being mineralized into dissolved inorganic carbon (Canfield, 1994). In contrast, biological Ba, existing mainly as $BaSO_4$, remains stable under oxic conditions but is prone to be decomposed and transported under reducing conditions (Anderson et al., 2002; McManus et al., 1998), while biogenic opal preservation is mainly controlled by diatom flux, with higher flux leading to better preservation and vice versa (Pondaven et al., 2000; Sayles et al., 2001). Therefore, to accurately constrain temporal variability of sea surface productivity, studies often utilize multiple indicators of export productivity simultaneously, as consistent trends between these indicators typically reflect changes in export productivity rather than preservation efficiency (e.g., Wu et al., 2017).

In addition to productivity records, some sediment cores have been analyzed for diatom assemblages to reconstruct environmental changes of, such as sea ice conditions with *Fragilariopsis curta*, and sea surface stratification with *Chaetoceros* Resting Spores (CRS), based on ecological habits of the diatom species (e.g., Li et al., 2021; Nie et al., 2022). Others have been surveyed for $\delta^{15}N$ in bulk sediment to reconstruct sea surface nitrate utilization efficiency (e.g., Hu et al., 2023).

3.3.2 *Bottom current strength and abyssal ventilation*

The strength of bottom currents in the Southern Ocean is primarily reconstructed using sediment grain-size compositions. Two methods can extract information about changes in bottom current intensity from grain-size data. The first is end-member modeling analyses (Jonkers et al., 2015; Prins et al., 2002), which decomposes grain-size distribution data to identify end-members that reflect hydrodynamic conditions, as demonstrated by Wu et al. (2018) and Wu et al. (2024). The second involves calculating the Sortable Silt Mean Grain-size (SSM) (McCave and Andrews, 2019; McCave et al., 2017). When SSM correlates linearly with the relative percentage of Sortable Silt (SS), it serves as a proxy for changes in bottom current strength (McCave and Andrews, 2019; McCave et al., 2017).

In addition, the geochemical ratio Zr/Rb provides an alternative method for reflecting the strength of bottom currents. This method, validated by Wu et al. (2020), has been successfully applied to high-resolution reconstructions of bottom current activity throughout the past 5 Ma in the South Pacific sector of the Southern Ocean (Lamy et al., 2024).

The redox state of bottom water masses is closely related to their ventilation status. During CHINARE, indicators such as manganese (Mn) and uranium (U) were used to assess this redox state (Wu et al., 2018; Wang et al., 2018, 2022a; Tang et al., 2022). In oxic conditions, Mn exists as Mn(Ⅲ) or Mn(Ⅳ) oxides/hydroxides, tending to precipitate and accumulate in sediments, and conversely, under reducing conditions, Mn is dissolved as Mn(Ⅱ)

ions, tending to dissolve and migrate (Calvert and Pedersen, 1993; Wagner and Hendy, 2017).

Similarly, in oxygen-rich environments, U is present as soluble U(Ⅵ). As oxygen levels decrease, U is reduced and precipitates as insoluble U(Ⅳ) (Morford and Emerson, 1999). This reduction creates a concentration gradient between the bottom water and the upper sediment layers, leading to the diffusion of dissolved U into the sediment and the formation of authigenic U phases (Morford and Emerson, 1999).

3.3.3 *Ice sheet/glaicer dynamics*

Ice-Rafted Debris (IRD) refers to terrestrial sediments transported by icebergs and deposited upon their melting, providing direct geological evidence of iceberg calving (Wang et al., 2013, 2023a). Icebergs can carry debris of various grain sizes, but sediments whose grain-size is <63 μm are often subject to sorting by ocean currents (McCave and Andrews, 2019). To account for this, IRD is typically defined as particles of grain-size >63 μm, or even coarser, to reduce the effects of current sorting, assuming that such larger sediment particles can not be moved by ocean currents (McCave and Andrews, 2019; Wang et al., 2013, 2023a; Liu et al., 2015). Core samples used to study iceberg activity and IRD include P1-3 (Liu et al., 2015), P1-2 (Wu et al., 2021), P5-03 (Wu et al., 2021), JB06 (Huang et al., 2016), and A2-10 (Wang et al., 2022b).

In addition, sediment provenance indicators are valuable for understanding glacier and ice sheet dynamics, as non-biogenic sediment components in the marginal seas around Antarctica primarily originate from erosion by AIS and glaciers (Cook et al., 2013; Hillenbrand et al., 2009; Wilson et al., 2018). Provenance indicators used in CHINARE cores include clay mineral compositions, Sr/Nd isotopic ratios (Wang et al., 2022b; Wu et al., 2021), and the geochemical composition of elements (Chen et al., 2024; Ge et al., 2022; Wang et al., 2022b; Zhang et al., 2023a).

4 Progress

4.1 *Surface seawater conditions evolution since the LGM*

The surface conditions in the high-latitude regions of the Southern Ocean are significantly influenced by sea ice, icebergs, and glacial melts (Li et al., 2021; Nie et al., 2022). These influences are authentically recorded through the composition of sedimentary diatom species and export productivity (Li et al., 2021; Nie et al., 2022). During the LGM, most marginal seas around Antarctica were either grounded by the marine portions of glaciers or covered by ice shelves and permanent sea ice, resulting in minimal export productivity (Hou et al., 1996, 1998; Xiu et al., 2017; Feng et al., 2023; Wu and Lu, 1998; Zhang et al., 2023b; Fan et al., 2021; Wang et al., 2014; Yan et al., 2023; Huang et al., 2016; Long et al., 2024). However, sediment Cores C3-09 and C4-05 from the Cosmonaut Sea, East Antarctica recorded a high abundance of *Fragilariopsis kerguelensis* (Fig. 2c), despite being close to the Antarctic continent (Table 1, Fig. 1). The presence of this open-ocean species, combined with relatively high level of *F. curta* (Fig. 2d), which indicates presence of winter sea ice (Gersonde and Zielinski, 2000), and *Actinocyclus actinochilus* (Fig. 2e), indicative of a cold-water environment (Esper et al., 2010, 2014), suggests that the area was covered only by seasonal sea ice even during the LGM (Li et al., 2021).

The LGM exhibits the highest abundance of CRS (Fig. 2b), relatively high *F. curta* (Fig. 2d) and *A. actinochilus* (Fig. 2f), and relatively low *F. kerguelensis* (Fig. 2c), indicating high seasonal sea ice density at the sites, with strong upper ocean stratification due to input of glacial melt water. During the last deglaciation, *F. curta* and *A. actinochilus* rapidly decreased while *F. kerguelensis* gradually increased, indicating a gradual reduction in seasonal sea ice cover at the sites. It is noteworthy that an increase in CRS and *F. curta* and a decrease in *F. kerguelensis* are prominent during Antarctic Cold Reversal (ACR), indicating millennial-scale rebound of seasonal sea ice cover in response to regional temperature drop (Fig. 2a). Throughout the Early and Mid-Holocene, the surface marine environment stabilized with minimal seasonal sea ice cover, possibly due to southward intrusion of CDW. Entering the Late Holocene, a trend of increasing seasonal sea ice cover at the sites emerged, accompanied by decreasing export productivity in this area (Hu et al., 2023).

Over the past 6 000 a, diatom records from Core D1-7 in the Bransfield Strait, West Antarctica, reveal exceptionally high levels of CRS (88%) (Fig. 3d) and low levels of *F. kerguelensis* (1.3%) (Fig. 3e). These findings contrast sharply with those at the Cosmonaut Sea sites. The high CRS content and low *F. kerguelensis* content suggest well-developed glacial meltwater and surface stratification, potentially due to greater dynamism of the West AIS compared to the East AIS. Additionally, the continuous presence of *F. curta* (Fig. 3f) and *F. kerguelensis* (Fig. 3e) indicates that the site has been persistently influenced by seasonal sea ice throughout the last 6 000 a. This is further supported by the occurrence of *Rhizosolenia antennata fo. semispina* (Fig. 3c) in the sediments, which suggests a cold or restricted open-water environment (Nie et al., 2022).

During the late Mid-Holocene, *Porosira glacialis*, which is associated with early sea ice advance and a strong presence of spring and winter sea ice, exhibited significantly lower and stable abundance compared to the Late Holocene (Nie et al., 2022). This stability in abundance, combined with the generally lower abundance ratio of *P. glacialis* to *Thalassiosira antarctica* (*P*/*T*) as shown in Fig. 3b, indicates a relatively less severe sea ice

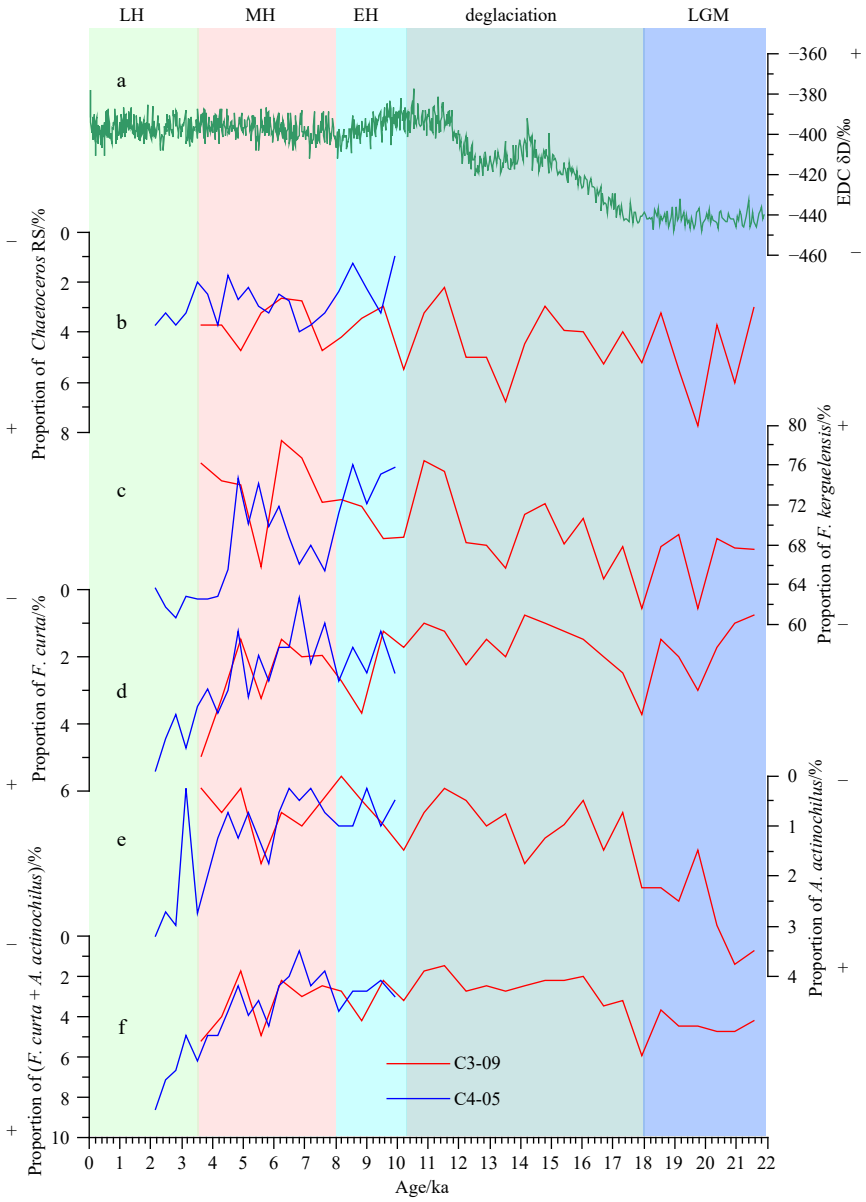


Fig. 2. Diatom records from Cosmonaut Sea Cores C3-09 and C4-05 according to Li et al. (2021). a. EDC δD (EPICA Community Members, 2004), b. *Chaetoceros* RS, c. *F. kerguelensis*, d. *F. curta*, e. *A. actinochilus*, f. *F. curta* + *A. actinochilus*. LH: Late Holocene. MH: Middle Holocene. EH: Early Holocene. Symbols + and − beside the vertical coordinates indicate increase and decrease of the values, respectively.

cover at the site and a more stable environmental condition compared to the Late Holocene.

Moving into the Late Holocene, the *P*/*T* ratio continues to increase, suggesting an increase in sea ice cover and surface water stratification. This trend aligns with the situation observed in the Cosmonaut Sea, as recorded by the export productivity (Fig. 3a) and diatom compositions (Fig. 2). Both areas exhibit synchronized evolution of the surface ocean environment, driven by local spring/summer solar radiation, intrusion of CDW, and cold water mass from beneath the Weddell Sea ice shelf (Li et al., 2021; Nie et al., 2022). However, the Bransfield Strait area, which faces the Pacific Ocean, may also be influenced by El Niño and Southern Oscillation activity (Nie et al., 2022).

4.2 *Export productivity and air-sea CO_2 exchange in glacial cycles*

The Southern Ocean is located at the rising branch of the North Atlantic overturning circulation, playing a crucial role in air-sea CO_2 exchange (Marshall and Speer, 2012). Physical, chemical, and biological processes within the Southern Ocean could regulate CO_2 distribution between the ocean and atmosphere efficiently, thereby impacting global climate (Abelmann et al., 2006; Elderfield and Rickaby, 2000; Ferrari et al., 2014; Sikes et al., 2023). The “biological pump” effect converts atmospheric CO_2 into organic matter, transferring it to deep-sea, while the “physical pump” effect pumps CO_2 from the deep Southern Ocean up to the upper/surface ocean where

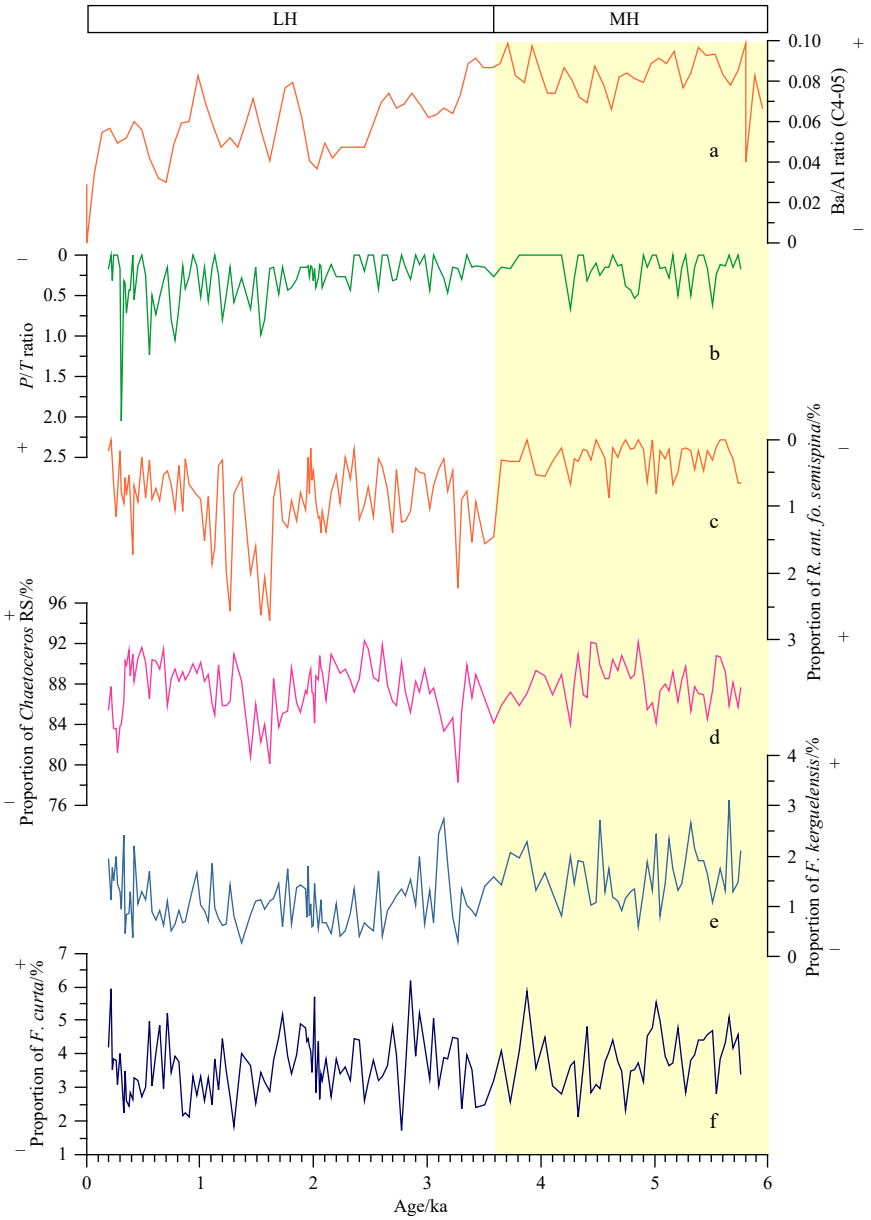


Fig. 3. Diatom records from the Bransfield Strait Core D1-7 (Nie et al., 2022). a. Export productivity record of the Cosmonaut Sea site C4-05 (Hu et al., 2022). b. *P*/*T* ratio. *P* represents the percent of *P. glacialis* and *T* represents percent of *T. antarctica*. c. *R. ant. fo. semispina*. d. *Chaetoceros* RS. e. *F. kerguelensis*. f. *F. curta*. Symbols + and – beside the vertical coordinates indicate increase and decrease of the values, respectively.

it exchanges with the atmosphere (Toggweiler et al., 2006).

The Southern Ocean's productivity is dominated by diatomaceous organisms contributed by diatoms (Cornet-Barthaux et al., 2007). On glacial-interglacial timescales, the growth of diatoms in the open ocean regions of the Southern Ocean is primarily influenced by nutrient supply, sourced mainly from upwelling of CDW (Anderson et al., 2009; Jaccard et al., 2013; Wu et al., 2017). Therefore, the export productivity in the open ocean area could reflect changes in the intensity of CDW upwelling (Anderson et al., 2009). In seasonal sea-ice zones, however, sea ice cover affects seawater stratification and availability of solar radiation, being another important factor influencing diatom growth (Presti et al., 2011; Wu et al., 2017). Most of the sediment cores collected during CHINARE are located in the seasonal sea-ice zones of the Southern Ocean (Fig. 1), contributing to the complexity of factors controlling productivity variability therein.

During the Middle to Late Quaternary, the Southern Ocean exhibits two modes of productivity variation on glacial-interglacial timescales (Jaccard et al., 2013). These variations typically co-vary with climate change, presenting a seesaw pattern between the north and the south of the APF. Specifically, during interglacials, higher productivity is observed south of the APF while it diminishes northward, and vice versa during glacials (Jaccard et al., 2013).

Many sediment cores collected during CHINARE surrounding Antarctica, including Prydz Bay (Wu et al., 2017), Amundsen Sea (Tang et al., 2022; Zhang et al., 2023b; Ju et al., 2019), Ross Sea (Long et al., 2024), and Scotia Sea, exhibit orbital-scale periodicity in export productivity evolution, characterized by higher export productivity in interglacials and lower in glacials, in phase with the temporal variations in the LR04-$\delta^{18}O$ stack (Lisiecki and Raymo, 2005) and EDC pCO_2 records (EPICA Community Members, 2004) (Fig. 4). The high interglacial productivity is attributed to the southward shift of the Southern Hemisphere westerlies, bringing more heat into high southern latitudes, resulting in ice sheet retreat, sea ice melting, enhanced CDW upwelling, and nutrient transfer into surface waters of the Southern Ocean (Anderson et al., 2009; Jaccard et al., 2013; Wu et al., 2017; Tang et al., 2022). Conversely, during glacials, the northward shift of the westerlies increases ice sheet extent and sea ice coverage, isolating seawater from the atmosphere, and weakening CDW upwelling, thereby transferring atmospheric CO_2 downward into the deep Southern Ocean through the biological pump (Anderson et al., 2009; Jaccard et al., 2013; Wu et al., 2017; Tang et al., 2022).

Interestingly, a comparison of the export productivity records from different marine regions reveals that during MIS 11 to MIS 6, or the so called Mid-Brunhes period (Barth et al., 2018; Wang et al., 2003; Yin and Berger, 2010), the glacial-interglacial oscillations of productivity seem to overlay a long-term increasing trend in productivity (Figs 4c–e). This sustained increase in productivity is seemingly parallel with the trend showing in the LR04 $\delta^{18}O$ stack (Fig. 4f) but was not found in lower latitude of the Southern Ocean (e.g., Jaccard et al., 2013) and may represent the response of the upper ocean environment in high-latitude Southern Ocean regions to Middle Pleistocene oceanic changes that is never identified before, warranting further investigation.

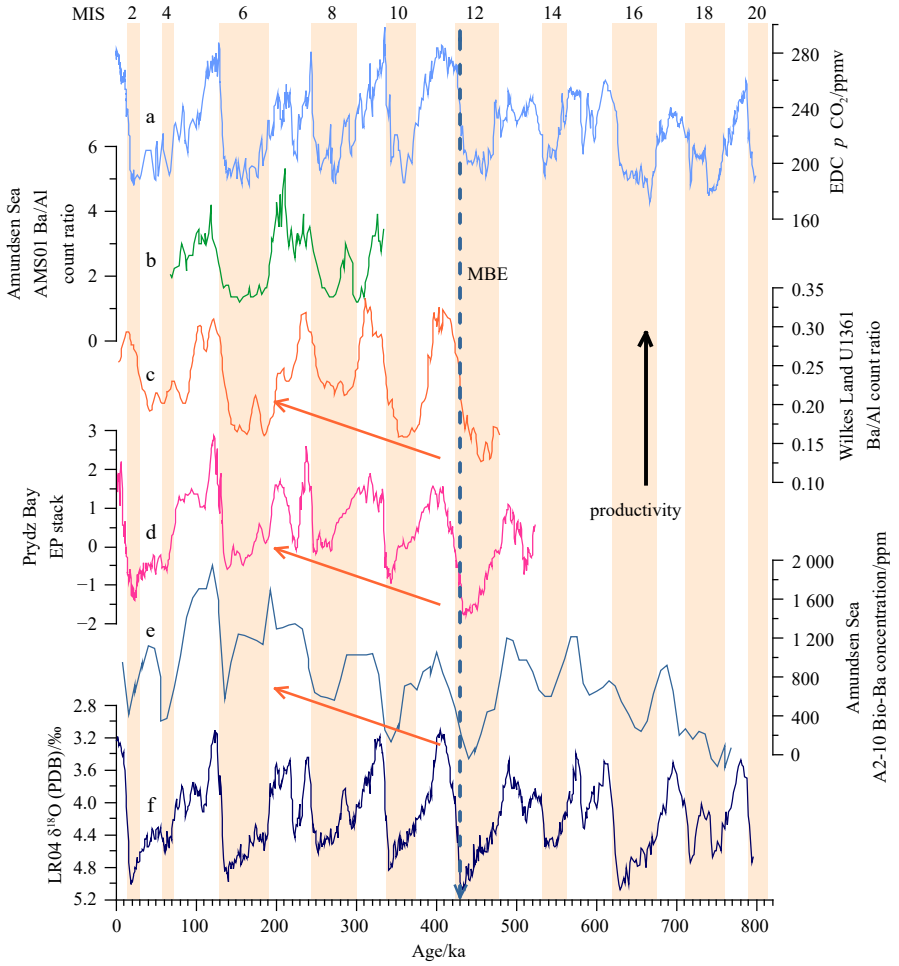


Fig. 4. A compilation of typical export productivity records around Antarctica. a. EDC pCO_2 (EPICA Community Members, 2004). b. Amundsen Sea AMS01 XRF scanning derived Ba/Al count ratio (Ju et al., 2019). c. XRF scanning derived Ba/Al count ratio of site U1361 from Wilkes Land (Wilson et al., 2018). d. Export Production (EP) stack from Prydz Bay (Wu et al., 2017). e. A2-10 biogenic Ba (Bio-Ba) from Amundsen Sea (Tang et al., 2022). f. LR04 $\delta^{18}O$ stack (Lisiecki and Raymo, 2005). The upward black arrow indicates increase in export productivity. The orange arrows indicate a long-term trend of export productivity increase from MIS 11 to MIS 6. The dotted downward arrow indicates the Mid-Brunhes Event (MBE). MIS: Marine Isotope Stage. PDB: Pee Dee Belemnite. ppm: 10^{-6}.

4.3 *Bottom water conditions and CO_2 storage in glacial cycles*

Some areas around Antarctica, including Cape Darnley, Wilkes Land, the western Ross Sea, and Weddell Sea, undergo processes of ice formation in sub-ice shelves and/or polynyas, generating high-density waters by brine rejection (Williams et al., 2008; Meijers et al., 2010). These brine passes over the continental shelf and slope, flows down submarine canyons, sinks into the depths of the Southern Ocean, and ultimately forms AABW, which carries dissolved oxygen into depths, filling and ventilating the bottom of the world's oceans (Foster and Carmack, 1976; Orsi et al., 1999; Williams et al., 2008; Yabuki et al., 2006).

Previous studies have found a close coupling between the physical and chemical properties of AABW and regional/global climate changes. Over millennial timescales, Jaccard et al. (2016) observed two-stage pulse-like elevation in dissolved oxygen concentration in the deep Weddell Sea during Heinrich Stadial 1 (HS1) and Younger Dryas (YD) (Jaccard et al., 2016). A CHINARE sediment core from Cosmonaut Sea recorded similar pulse-like elevation in abyssal ventilation during the last deglacial period (Hu et al., 2023). During glacial periods, the rate of formation of bottom waters in Weddell Sea significantly decreased, although there were probably some millennial-scale strengthened bottom current activities (Yan et al., 2023), in response to temporary southward shift of the southern westerly wind belt (Lu et al., 2022). In particular, during glacial maxima, northward export of AABW from the Weddell Sea nearly stagnated (Huang et al., 2020).

On glacial-interglacial timescales, sediment cores off Prydz Bay recorded that each deglaciation of the Late Quaternary was always accompanied by intense authigenic Mn enrichment (Fig. 5c) (Li et al., 2022; Wu et al., 2018), elevated silt relative to clay (S2/S1) (Fig. 5b) as well as Zr/Rb ratio (Wu et al., 2018, 2020), indicating enhanced diapycnal mixing and ventilation in the deep Southern Ocean (Wu et al., 2018). This process might lead to continuous diffusion of deeply sequestered CO_2 mixing upward, facilitating its transfer to the upper ocean and ultimately release into the atmosphere, and consequently a sudden increase in atmospheric CO_2 during deglaciations (Fig. 5a; Wu et al., 2018). This interpretation is also supported by the strong Mn enrichment during the recent four deglacial periods in sediment cores collected off Wilkes Land (Jimenez-Espejo et al., 2020).

In another work, Tang et al. (2022) further found co-variation of Mn enrichment (Fig. 5d) and authigenic uranium (aU) enrichment (Fig. 5e) on glacial-interglacial timescales in the sediment Core A2-10 from the Amundsen Sea over the last 770 ka, showing higher authigenic Mn enrichment and lower authigenic aU during interglacial, and lower authigenic Mn enrichment and higher authigenic aU during interglacials. They interpreted this co-variation as a compensation relationship between deep Southern Ocean dissolved oxygen content and abyssal carbon storage (Tang et al., 2022). Specifically, during glacial period, dissolved oxygen concentration in the abyssal Southern Ocean decreased while carbon storage increased, and vice versa during interglacials, resulting in continuous switching of the Southern Ocean between a carbon sink and a carbon source during glacial-interglacial cycles (Tang et al., 2022).

4.4 *AIS dynamics in glacial cycles*

AIS/glacier dynamics are directly related to global sea level fluctuations (Blackburn et al., 2020; DeConto and Pollard, 2016). Under the background of global warming, Antarctic glaciers are showing an accelerating trend of melting (Pattyn et al., 2018). The historical patterns and mechanisms of AIS fluctuations have significant implications for predicting its future dynamics, and have been receiving increasing attention (Hillenbrand et al., 2009; Pollard and DeConto, 2009; Wilson et al., 2018; Wu et al., 2021).

Measurements of submarine topography and seismic profiles on the Antarctic continental shelf provide direct geological evidence of the extent of Antarctic glacier fluctuations (Domack et al., 1998; O'Brien et al., 1999). These studies indicate the presence of extensive glacial erosion features across the Antarctic continental shelf during the LGM, indicating northward advance of Antarctic glaciers (Anderson et al., 2014b; Domack et al., 1998; Halberstadt et al., 2016; O'Brien et al., 1999; Prothro et al., 2018). During the last deglacial period, these glaciers rapidly retreated, transforming the continental shelf from a sub-glacial/sub-ice shelf environment to a seasonal open ocean environment. Some of the glaciers' grounding lines did not retreat to their near-modern positions until the Late Holocene (Anderson et al., 2014b; Prothro et al., 2020).

Glacier retreat on the continental shelf triggered a series of oceanic environmental changes. For instance, during the last glacial period, Yan et al. (2023) found deposition of IRD in the northwest of the Weddell Sea was closely related to strengthening of local bottom currents, and a series of studies (Zhao et al., 2017; Huang et al., 2016; Fan et al, 2021; Liu et al., 2024) observed diminished bottom current strength in the central and western Ross Sea shelves as glaciers retreated, accompanied by significant increases in IRD deposition. During the last deglacial period, Zhang et al. (2023a) and Chen et al. (2024) found that sedimentary process in Cosmonaut Sea was controlled by changes in the dynamics of the Lambert Glacier system in Prydz Bay in the east, and may align closely with millennial-scale climate fluctuations (Chen et al., 2024; Zhang et al., 2023a). Moving to Holocene, Lei et al. (2022) discovered that the deposition of IRD in Amundsen Sea decreased with gradually declining local atmospheric temperatures (Lei et al., 2022).

On glacial-interglacial timescales, deep sea sediment cores from the Prydz Bay sector and the Amundsen Sea sector recorded the dynamic changes of the Lambert

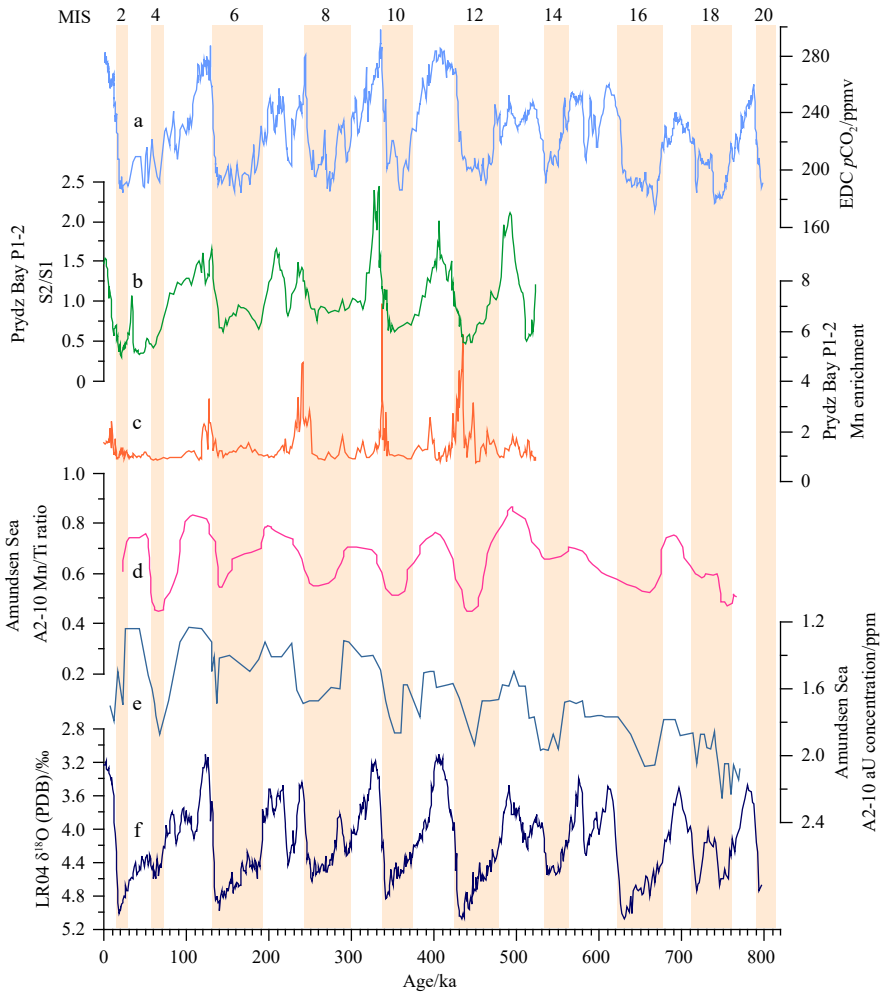


Fig. 5. Abyssal ventilation records in the Prydz Bay sector- and the Amundsen Sea sector-Southern Ocean compared with patterns of global climate fluctuations on glacial-interglacial timescales. a. EDC pCO_2 (EPICA Community Members, 2004). b. Prydz Bay Core P1-2 S2/S1 (Wu et al., 2018). S1 and S2 refer to sensitive grain-size intervals 9.82−27.4 μm and 1.52−2.92 μm, respectively. c. Prydz Bay Core P1-2 Mn enrichment index (Wu et al., 2018). d. Amundsen Sea Core A2-10 Mn/Ti ratio (Tang et al., 2022). e. Amundsen Sea Core A2-10 authigenic U (aU) (Tang et al., 2022). f. LR04 $\delta^{18}O$ stack (Lisiecki and Raymo, 2005). MIS: Marine Isotope Stage. PDB: Pee Dee Belemnite.

Glacier system (Ge et al., 2022; Liu et al., 2015; Wu et al., 2021) and the glaciers around the West AIS (Wang et al., 2022b). IRD records of these cores provide direct evidence for the dynamics of the glaciers (Liu et al., 2015), while clay mineral compositions in these cores provide a more detailed history of their fluctuations (Wang et al., 2022b; Wu et al., 2021).

During interglacial periods, the clay mineral composition of the Prdzy Bay Cores P1-2 and P5-3 is dominated by an illite-rich end member (EM1), whereas in glacial periods, it is dominated by a kaolinite-rich end member (EM2). EM1 was interpreted as a background sedimentation of clay minerals, while EM2 was likely derived from older successions in the Prydz continental shelf due to reworking of the Lamber Glacier system, and thus EM2/(EM1 + EM2) was used to represent the relative position of the grounding line of the Lambert Glacier in geological history (Fig. 6c; Wu et al., 2021). This index exhibits a temporal variation pattern similar to deep-sea oxygen isotopes (Fig. 6g; Lisiecki and Raymo, 2005) and Antarctic ice volume changes (Fig. 6a; Pollard and DeConto, 2009) over glacial-interglacial timescales, indicating the sensitivity of the Lambert Glacier system to oceanic forcing and sea level changes (Wu et al., 2021). Nd isotopes show that besides the north-south advance and retreat of the Lambert Glacier system, there may also be lateral readjustment of the glacier system during MIS 12 and MIS 4−2 (Fig. 6d), possibly in response to eccentricity minima (Ge et al., 2022).

In the Amundsen Sea region, the source rocks of illite and chlorite might be widely distributed in Antarctica and thus serve as background sedimentation as well, while kaolinite is primarily supplied from subglacial erosion of pre-Oligocene sedimentary rocks or palaeosoils in the hinterland of Amundsen Sea (Hillenbrand et al., 2002, 2003), and smectite may be derived from Cenozoic volcanic rocks in Marie Byrd Land (Hillenbrand et al., 2003). Kaolinite content in the sediments might be related to dy-

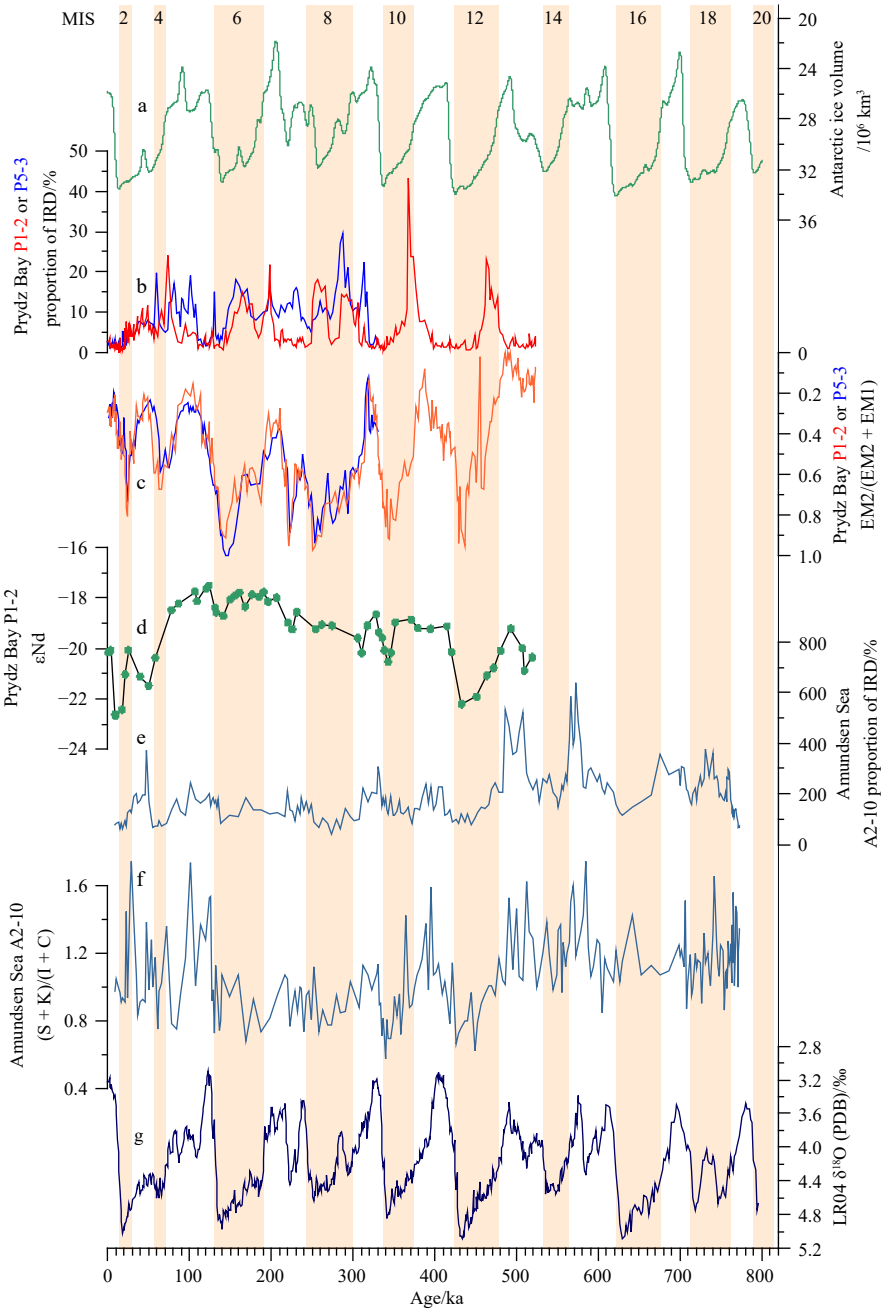


Fig. 6. A comparison of proxy records for dynamics of glaciers in the Prydz Bay sector- and the Amundsen Sea sector-Southern Ocean. a. Modelled Antarctic ice volume (Pollard and DeConto). b. Prydz Bay Cores P1-2 and P5-3 IRD records (Wu et al., 2021). c. Prydz Bay Cores P1-2 and P5-3 clay mineral end member ratio EM2/(EM2 + EM1) (Wu et al., 2021). EM1 is an illite-rich end member and EM2 is kaolinite-rich. d. Prydz Bay Core P1-2 εNd (Ge et al., 2022). e. Amundsen Sea Core A2-10 IRD record (the 150−2 000 μm fractions) (Wang et al., 2022b). f. Amundsen Sea Core A2-10 clay mineral composition ratio (smectite + kaolinite)/(illite + chlorite) [(S + K)/(I + C)] (Wang et al., 2022b). g. LR04 $\delta^{18}O$ stack (Lisiecki and Raymo, 2005). MIS: Marine Isotope Stage. The orange shades indicate glacial periods. PDB: Pee Dee Belemnite.

namical behaviour of the glaciers in the Amundsen Sea sector, as recorded in sediment Core PS5458/254 from the continental rise (Hillenbrand et al., 2009).

In further north at the Core A2-10, changes of the current system in the Southern Ocean might play a more significant role in regulating the composition of clay minerals (Wang et al., 2022b), and the ratio (smectite + kaolinite)/(illite + chlorite) in Core A2-10 was used as a proxy for the relative strength of the ACC and the Antarctic Slope Current. However, it indirectly indicated waxing and waning of the glacier systems around the Amundsen Sea sector, West Antarctica (Fig. 6f; Wang et al., 2022b). Higher values during interglacial periods indicate more influence from the ACC, implying a retreated glacier system in the Amundsen Sea sector, and during glacial period, lower values indicate more influence form the Antarc-

tic Slope Current, hinting an expanded glacier system (Wang et al., 2022b).

Overall, similar glacial-interglacial variation pattern of the glacier systems in the Prydz Bay sector and the Amundsen Sea sector (Figs 6c and f) indicates oceanic forcing was the primary forcing mechanism for the dynamics of the marine-based ice sheet in both East Antarctica and West Antarctica during the middle to late Pleistocene (Ge et al., 2022; Wang et al., 2022b; Wu et al., 2021). Interestingly, however, IRD occurrence recorded in these sediment cores differ. In the Prydz Bay cores, IRD were mainly present during interglacial-to-glacial transitions (Fig. 6b), while in Amundsen Sea, IRD were predominantly present in interglacial periods (Fig. 6e), consistent with the temporal distribution of the (smectite + kaolinite)/(illite + chlorite) ratio (Fig. 6f), possibly indicating different scenarios of iceberg calving in these areas, and also reminding that caution must be paid when correlating IRD records with a fixed phase of ice sheet/glacier evolution in the Southern Ocean.

5 Summary

In this review, we compiled studies on paleoceanographic and paleoclimatic changes recorded in sediments from the high-latitude Southern Ocean during the Middle to Late Pleistocene based on CHINARE data. The major findings are summarized as follows.

(1) Diatom compositions and sea surface conditions: Diatom records indicate changes in sea surface conditions since the LGM in Bransfield Strait, West Antarctica, and Cosmonaut Sea, East Antarctica. Despite their long distance from each other, both areas show an increase in sea ice cover since the end of the Mid-Holocene, potentially related to reduced local insolation and cold water mass injection from beneath the Weddell Sea ice shelf. Additionally, a polynya may have existed in the Cosmonaut Sea area during the LGM.

(2) Export productivity: Records of export productivity around Antarctica reveal a consistent glacial-interglacial variation pattern, with higher productivity during interglacial periods and lower productivity during glacial periods. This pattern is influenced by both the intensity of CDW upwelling and sea ice cover. Notably, there is an observed long-term increase in export productivity from MIS 12 to MIS 6 in different sectors of the high latitudes of the Southern Ocean, responding to the amplification of the polar climate since MBE (about 430 ka).

(3) Ventilation state of the Abyssal Southern Ocean: The ventilation state of the abyssal Southern Ocean is closely linked to global climate change and atmospheric CO_2 concentrations. Increased ventilation efficiency during deglacial periods might be partly responsible for elevated atmospheric CO_2 levels, while varying ventilation efficiency during interglacial and glacial periods partly explains the fluctuations in atmospheric CO_2 concentrations during these times.

(4) Ice sheets/glaciers dynamics: Marine-based ice sheets and glaciers in Antarctica exhibit fluctuations in alignment with global and (simulated) regional ice volume changes on glacial-interglacial timescales, predominantly influenced by oceanic forcing. In contrast, terrestrial ice sheets, particularly in the Prydz Bay region, appear to have been reorganized mainly during specific glacial intervals, such as MIS 12 and MIS 4−2.

6 Future perspective

This review demonstrates that substantial progress has been achieved through CHINARE over the past 40 years in understanding the role of the Southern Ocean and the AIS within the global climate system. Nonetheless, several challenges persist, including:

(1) Sample collection: Although CHINARE has extensively covered important sectors of the Southern Ocean, the focus has primarily been on regions south of 65°S within the seasonal sea ice zone. Furthermore, the core lengths (less than about 8.2 m) and temporal spans (<770 ka) of samples are generally limited. Additionally, other critical frontal zones, such as the SPF zone, which are essential for studying changes in the Southern Hemisphere westerlies and CDW upwelling, remain underrepresented. Future studies should, therefore, aim to collect samples from a wider range of latitudes and ensure these samples are of higher quality and span a longer temporal range.

(2) Research methods: First, the dating of marine sediments from high-latitude regions of the Southern Ocean remains unresolved. Recent advancements, including the introduction of Relative PaleoIntensity (RPI) (e.g., Ge et al., 2014; Hopkins et al., 2024) and the compound specific AMS^{14}C dating (e.g., Prothro et al., 2020) methods, offer promising solutions. Second, there is still a lack of comprehensive records for seawater temperature reconstruction in these high-latitude regions. While biomarkers (e.g., Chen et al., 2021) and foraminifera-based proxies (e.g., Song et al., 2022) have been used to attempt sea surface temperature reconstructions, further calibration is necessary. Additionally, the Southern Ocean plays a critical role in ocean-atmosphere CO_2 exchange, but direct geological reconstructions of carbon cycling (such as using foraminifer-based boron isotope and B/Ca ratio) in the intermediate to deep water masses in this region are limited, highlighting a crucial aspect for future research.

Acknowledgements

We thank the CHINARE cruise members for retrieving the sediments and Polar Research Center of China for providing the sediment samples. We are also grateful to authors who have provided us with data on request or via online repositories.

References

Abelmann A, Gersonde R, Cortese G, et al. 2006. Extensive phytoplankton blooms in the Atlantic sector of the glacial Southern Ocean. Paleoceanography, 21(1): PA1013, doi: 10.1029/2005PA001199

An Zhisheng, Zhou Weijian, Zhang Zeke, et al. 2024. Mid-Pleistocene climate transition triggered by Antarctic Ice Sheet growth. Science, 385(6708): 560–565, doi: 10.1126/science.abn4861

Anderson R F, Ali S, Bradtmiller L I, et al. 2009. Wind-driven upwelling in the Southern Ocean and the deglacial rise in atmospheric CO_2. Science, 323(5920): 1443–1448, doi: 10.1126/science.1167441

Anderson R F, Barker S, Fleisher M, et al. 2014a. Biological response to millennial variability of dust and nutrient supply in the Subantarctic South Atlantic Ocean. Philosophical Transactions of the Royal Society A: Mathematical, Physical and Engineering Sciences, 372(2019): 20130054, doi: 10.1098/rsta.2013.0054

Anderson R F, Chase Z, Fleisher M Q, et al. 2002. The Southern Ocean's biological pump during the last glacial maximum. Deep-Sea Research Part Ⅱ: Topical Studies in Oceanography, 49(9–10): 1909–1938, doi: 10.1016/S0967-0645(02)00018-8

Anderson J B, Conway H, Bart P J, et al. 2014b. Ross Sea paleo-ice sheet drainage and deglacial history during and since the LGM. Quaternary Science Reviews, 100: 31–54, doi: 10.1016/j.quascirev.2013.08.020

Barth A M, Clark P U, Bill N S, et al. 2018. Climate evolution across the Mid-Brunhes transition. Climate of the Past, 14(12): 2071–2087, doi: 10.5194/cp-14-2071-2018

Blackburn T, Edwards G H, Tulaczyk S, et al. 2020. Ice retreat in Wilkes Basin of East Antarctica during a warm interglacial. Nature, 583(7817): 554–559, doi: 10.1038/s41586-020-2484-5

Bonn W J, Gingele F X, Grobe H, et al. 1998. Palaeoproductivity at the Antarctic continental margin: opal and barium records for the last 400 ka. Palaeogeography, Palaeoclimatology, Palaeoecology, 139(3–4): 195–211, doi: 10.1016/S0031-0182(97)00144-2

Bostock H C, Barrows T T, Carter L, et al. 2013. A review of the Australian–New Zealand sector of the Southern Ocean over the last 30 ka (Aus-INTIMATE project). Quaternary Science Reviews, 74: 35–57, doi: 10.1016/j.quascirev.2012.07.018

Calvert S E, Pedersen T F. 1993. Geochemistry of recent oxic and anoxic marine sediments: implications for the geological record. Marine Geology, 113(1–2): 67–88, doi: 10.1016/0025-3227(93)90150-T

Canfield D E. 1994. Factors influencing organic carbon preservation in marine sediments. Chemical Geology, 114(3–4): 315–329, doi: 10.1016/0009-2541(94)90061-2

Chen Dong, Ge Qian, Lei Ziyan, et al. 2024. Glacial activity and paleoclimatic evolution records in the Cosmonaut Sea since the last glacial maximum. Frontiers in Marine Science, 11: 1379673, doi: 10.3389/fmars.2024.1379673

Chen Xin, Liu Xiaodong, Lin Dacheng. et al. 2021. A potential suite of climate markers of long-chain *n*-alkanes and alkenones preserved in the top sediments from the Pacific sector of the Southern Ocean. Progress in Earth and Planetary Science, 8(1): 23, doi: 10.1186/s40645-021-00416-9

Comiso J C. 2010. Variability and trends of the global sea ice cover. In: Thomas D N, Dieckmann G S, eds. Sea Ice. Oxford: Blackwell Publishing Ltd, 205–246, doi: 10.1002/9781444317145.ch6

Cook C P, van de Flierdt T, Williams T, et al. 2013. Dynamic behaviour of the East Antarctic ice sheet during Pliocene warmth. Nature Geoscience, 6(9): 765–769, doi: 10.1038/ngeo1889

Cornet-Barthaux V, Armand L, Quéguiner B. 2007. Biovolume and biomass estimates of key diatoms in the Southern Ocean. Aquatic Microbial Ecology, 48: 295–308, doi: 10.3354/ame048295

Crosta X, Pichon J J, Burckle L H. 1998. Reappraisal of Antarctic seasonal sea-ice at the Last Glacial Maximum. Geophysical Research Letters, 25(14): 2703–2706, doi: 10.1029/98GL02012

DeConto R M, Pollard D. 2016. Contribution of Antarctica to past and future sea-level rise. Nature, 531(7596): 591–597, doi: 10.1038/nature17145

Domack E, Leventer A, Dunbar R, et al. 2001. Chronology of the Palmer Deep site, Antarctic Peninsula: a Holocene palaeoenvironmental reference for the circum-Antarctic. The Holocene, 11(1): 1–9, doi: 10.1191/095968301673881493

Domack E, O'Brien P, Harris P, et al. 1998. Late Quaternary sediment facies in Prydz Bay, East Antarctica and their relationship to glacial advance onto the continental shelf. Antarctic Science, 10(3): 236–246, doi: 10.1017/S0954102098000339

Elderfield H, Rickaby R E M. 2000. Oceanic Cd/P ratio and nutrient utilization in the glacial Southern Ocean. Nature, 405(6784): 305–310, doi: 10.1038/35012507

EPICA Community Members. 2004. Eight glacial cycles from an Antarctic ice core. Nature, 429(6992): 623–628, doi: 10.1038/nature02599

Esper O, Gersonde R. 2014. Quaternary surface water temperature estimations: New diatom transfer functions for the Southern Ocean. Palaeogeography, Palaeoclimatology, Palaeoecology, 414: 1–19, doi: 10.1016/j.palaeo.2014.08.008

Esper O, Gersonde R, Kadagies N. 2010. Diatom distribution in southeastern Pacific surface sediments and their relationship to modern environmental variables. Palaeogeography, Palaeoclimatology, Palaeoecology, 287: 1–27, doi: 10.1016/j.palaeo.2009.12.006

Fan Jiaen, Wang Rujian, Ding Xuan, et al. 2021. Benthic foraminifera assemblages and their response to ice shelf changes in the joides through of the Ross Sea, Antarctica since the last glacial period. Journal of Micropalaeontology (in Chinese), 38(1): 93–111

Feng Zongbao, Chen Zhihua, Yang Chunli, et al. 2023. Sediment provenances and environmental changes in the southeastern Scotia Sea, Antarctica, since the Last Glaciation. Haiyang Xuebao (in Chinese), 45(7): 56–68, doi: 10.12284/hyxb2023105

Ferrari R, Jansen M F, Adkins J F, et al. 2014. Antarctic sea ice control on ocean circulation in present and glacial climates. Proceedings of the National Academy of Sciences of the United States of America, 111(24): 8753–8758, doi: 10.1073/pnas.1323922111

Foster T D, Carmack E C. 1976. Frontal zone mixing and Antarctic Bottom water formation in the southern Weddell Sea. Deep-Sea Research and Oceanographic Abstracts, 23(4): 301–317, doi: 10.1016/0011-7471(76)90872-X

Fretwell P, Pritchard H D, Vaughan D G, et al. 2013. Bedmap2: improved ice bed, surface and thickness datasets for Antarctica. The Cryosphere, 7(1): 375–393, doi: 10.5194/tc-7-375-2013

Ge Shulan, Chen Zhihua, Liu Jianxing, et al. 2014. Dating sediment core by relative paleointensity and direction of geomagnetic field in Bransfield Strait, Antarctic Peninsula. Chinese Journal of Polar Research (in Chinese), 26(1): 98–110, doi: 10.13679/j.jdyj.2014.1.098

Ge Shulan, Chen Zhihua, Liu Qingsong, et al. 2022. Dynamic response of East Antarctic ice sheet to Late Pleistocene glacial–interglacial climatic forcing. Quaternary Science Reviews, 277: 107299, doi: 10.1016/j.quascirev.2021.107299

Gersonde R, Crosta X, Abelmann A, et al. 2005. Sea-surface temperature and sea ice distribution of the Southern Ocean at the EPILOG Last Glacial Maximum—a circum-Antarctic view based on siliceous microfossil records. Quaternary Science Reviews, 24(7–9): 869–896, doi: 10.1016/j.quascirev.2004.07.015

Gersonde R, Zielinski U. 2000. The reconstruction of late Quaternary Antarctic sea-ice distribution-the use of diatoms as a proxy for sea-ice. Palaeogeography, Palaeoclimatology, Palaeoecology, 162(3–4): 263–286, doi: 10.1016/S0031-0182(00)00131-0

Golledge N R, Levy R H, McKay R M, et al. 2017. East Antarctic ice sheet most vulnerable to Weddell Sea warming. Geophysical Research Letters, 44(5): 2343–2351, doi: 10.1002/2016GL072422

Gu Senchang, Yan Wen. 1997. A preliminary study on the element strata and palaeoenvironment of core NP951 from the Prydz Bay, Antarctica. Chinese Journal of Polar Research, 9(2): 112–118.

Hajdas I, Ascough P, Garnett M H, et al. 2021. Radiocarbon dating. Nature Reviews Methods Primers, 1: 62, doi: 10.1038/s43586-021-00058-7

Halberstadt A R W, Simkins L M, Greenwood S L, et al. 2016. Past ice-sheet behaviour: retreat scenarios and changing controls in the Ross Sea, Antarctica. The Cryosphere, 10(3): 1003–1020, doi: 10.5194/tc-10-1003-2016

Hillenbrand C D, Fütterer D, Grobe H, et al. 2002. No evidence for a Pleistocene collapse of the West Antarctic Ice Sheet from continental margin sediments recovered in the Amundsen Sea. Geo-Marine Letters, 22(2): 51–59, doi: 10.1007/s00367-002-0097-7

Hillenbrand C D, Grobe H, Diekmann B, et al. 2003. Distribution of clay minerals and proxies for productivity in surface sediments of the Bellingshausen and Amundsen seas (West Antarctica)-relation to modern environmental conditions. Marine Geology, 193(3–4): 253–271, doi: 10.1016/S0025-3227(02)00659-X

Hillenbrand C D, Kuhn G, Frederichs T. 2009. Record of a Mid-Pleistocene depositional anomaly in West Antarctic continental margin sediments: an indicator for ice-sheet collapse?. Quaternary Science Reviews, 28(13–14): 1147–1159, doi: 10.1016/j.quascirev.2008.12.010

Hopkins B, Xuan C, Hillenbrand C D, et al. 2024. Evaluation of geomagnetic relative palaeointensity as a chronostratigraphic tool in the Southern Ocean: refined Plio-/Pleistocene chronology of IODP Site U1533 (Amundsen Sea, West Antarctica). Quaternary Science Reviews, 325: 108460, doi: 10.1016/j.quascirev.2023.108460

Hou Hongming, Luo Youlang, Zheng Honghan, et al. 1998. Heinrich layer in Antarctic marine sediments and its significance to global changes. Chinese Science Bulletin (in Chinese), 43(21): 1830–1834, doi: 10.1007/BF02883383

Hou Hongming, Wang Baogui, Tang Xianzan. 1996. Magnetic fabric characteristic of core NP93-2 from Prydz Bay, Antarctica and its paleoclimatic significance. Journal of Geophysics (in Chinese), 39(6): 747–752

Hu Benchao, Long Feijiang, Han Xibin, et al. 2022. The evolution of paleoproductivity since the Middle Holocene in the Cosmonaut Sea, Antarctic. Earth Science Frontiers (in Chinses), 29(4): 113–122, doi: 10.13745/j.esf.sf.2022.1.12

Hu Liangming, Zhang Yi, Wang Yizhou, et al. 2023. Paleoproductivity and deep-sea oxygenation in Cosmonaut Sea since the last glacial maximum: impact on atmospheric CO_2. Frontiers in Marine Science, 10: 1215048, doi: 10.3389/fmars.2023.1215048

Huang H, Gutjahr M, Eisenhauer A, et al. 2020. No detectable Weddell Sea Antarctic bottom water export during the last and penultimate glacial maximum. Nature Communications, 11(1): 424, doi: 10.1038/s41467-020-14302-3

Huang Mengxue, Wang Rujian, Xiao Wenshen, et al. 2016. Retreat process of Ross ice shelf and hydrodynamic changes on northwestern Ross continental shelf since the last glacial. Marine Geology & Quaternary Geology (in Chinese), 36(5): 97–108, doi: 10.16562/j.cnki.0256-1492.2016.05.010

Jaccard S L, Galbraith E D, Martínez-García A, et al. 2016. Covariation of deep Southern Ocean oxygenation and atmospheric CO_2 through the last ice age. Nature, 530(7589): 207–210, doi: 10.1038/nature16514

Jaccard S L, Galbraith E D, Sigman D M, et al. 2010. A pervasive link between Antarctic ice core and subarctic Pacific sediment records over the past 800kyrs. Quaternary Science Reviews, 29(1–2): 206–212, doi: 10.1016/j.quascirev.2009.10.007

Jaccard S L, Hayes C T, Martínez-García A, et al. 2013. Two modes of change in Southern Ocean productivity over the past million years. Science, 339(6126): 1419–1423, doi: 10.1126/science.1227545

Jimenez-Espejo F J, Presti M, Kuhn G, et al. 2020. Late Pleistocene oceanographic and depositional variations along the Wilkes Land margin (East Antarctica) reconstructed with geochemical proxies in deep-sea sediments. Global and Planetary Change, 184: 103045, doi: 10.1016/j.gloplacha.2019.103045

Jonkers L, Barker S, Hall I R, et al. 2015. Correcting for the influence of ice-rafted detritus on grain size-based paleocurrent speed estimates. Paleoceanography, 30(10): 1347–1357, doi: 10.1002/2015PA002830

Ju Mengshan, Chen Zhihua, Zhao Renjie, et al. 2019. Late Quaternary cyclic variations of ice sheet and paleoproductivity in the Amundsen Sea sector, Antarctica. Haiyang Xuebao (in Chinese), 41(9): 40–51, doi: 10.3969/j.issn.0253-4193.2019.09.004

Lamy F, Winckler G, Arz H W, et al. 2024. Five million years of Antarctic Circumpolar Current strength variability. Nature, 627(8005): 789–796, doi: 10.1038/s41586-024-07143-3

Lei Ziyan, Ge Qian, Chen Dong, et al. 2022. Provenance of sediments in the Amundsen Sea, West Antarctic since the mid-Holocene and paleoclimate reconstruction. Frontiers in Geology (in Chinese), 29(4): 179–190, doi: 10.13745/j.esf.sf.2022.1.7

Li Guogang, Bu Ruyuan, Yi Liang, et al. 2022. Geochronology and Paleoenvironmental changes of Late Pleistocene sediments in the Ross Sea, Antarctica. Frontiers in Earth Science, 10: 863336, doi: 10.3389/feart.2022.863336

Li Qingmiao, Xiao Wenshen, Wang Rujian, et al. 2021. Diatom based reconstruction of climate evolution through the Last Glacial Maximum to Holocene in the Cosmonaut Sea, East Antarctica. Deep-Sea Research Part Ⅱ: Topical Studies in Oceanography, 194: 104960, doi: 10.1016/j.dsr2.2021.104960

Lisiecki L E, Raymo M E. 2005. A Pliocene-Pleistocene stack of 57 globally distributed benthic $\delta^{18}O$ records. Paleoceanography, 20(1): PA1003, doi: 10.1029/2004PA001071

Liu Helin, Chen Zhihua, Ge Shulan, et al. 2015. Late Quaternary sedimentary records and paleoceanographic implications from the core on continental slope off the Prydz Bay, east Antarctic. Marine Geology & Quaternary Geology (in Chinese), 35(3): 209–217, doi: 10.3724/SP.J.1140.2015.03209

Liu Geng, Shen Zhongshan, Han Xibin, et al. 2024. Chronology and sedimentary processes in the Western Ross Sea, Antarctica since the Last Glacial period. Marine Science and Engineering, 12(2): 254, doi: 10.3390/jmse12020254

Long Feijiang, Xiang Bo, Wang Yizhuo, et al. 2024. Evolution of paleoproductivity in the Antarctica Ross Sea since the Last Glacial Maximum. Marine Geology & Quaternary Geology (in Chinese), 44(1): 109–120, doi: 10.16562/j.cnki.0256-1492.2022111601

Lu Lijuan, Zheng Xufeng, Chen Zhong, et al. 2022. One-to-one coupling between Southern Ocean productivity and Antarctica climate. Geophysical Research Letters, 49(13): e2022GL098761, doi: 10.1029/2022GL098761

Marshall J, Speer K. 2012. Closure of the meridional overturning circulation through Southern Ocean upwelling. Nature Geoscience, 5(3): 171–180, doi: 10.1038/ngeo1391

Martínez-Garcia A, Rosell-Melé A, Jaccard S L, et al. 2011. Southern Ocean dust-climate coupling over the past four million years. Nature, 476(7360): 312–315, doi: 10.1038/nature10310

McCave I N, Andrews J T. 2019. Distinguishing current effects in sediments delivered to the ocean by ice. Ⅰ. Principles, methods and examples. Quaternary Science Reviews, 212: 92–107, doi: 10.1016/j.quascirev.2019.03.031

McCave I N, Thornalley D J R, Hall I R. 2017. Relation of sortable silt grain-size to deep-sea current speeds: calibration of the 'Mud Current Meter'. Deep-Sea Research Part Ⅰ: Oceanographic Research Papers, 127: 1–12, doi: 10.1016/j.dsr.2017.07.003

McManus J, Berelson W M, Klinkhammer G P, et al. 1998. Geochemistry of barium in marine sediments: Implications for its use as a paleoproxy. Geochimica et Cosmochimica Acta, 62(21–22): 3453–3473, doi: 10.1016/S0016-7037(98)00248-8

Meckler A N, Sigman D M, Gibson K A, et al. 2013. Deglacial pulses of deep-ocean silicate into the subtropical North Atlantic Ocean. Nature, 495(7442): 495–498, doi: 10.1038/nature12006

Meijers A J S, Klocker A, Bindoff N L, et al. 2010. The circulation and water masses of the Antarctic shelf and continental slope between 30 and 80°E. Deep-Sea Research Part Ⅱ: Topical Studies in Oceanography, 57(9–10): 723–737, doi: 10.1016/j.dsr2.2009.04.019

Morford J L, Emerson S. 1999. The geochemistry of redox sensitive trace metals in sediments. Geochimica et Cosmochimica Acta, 63(11–12): 1735–1750, doi: 10.1016/S0016-7037(99)00126-X

Nie Senyan, Wang Rujian, Xiao Wenshen. 2014. A 6000-year record of terrigeneous components from the Bransfield Strait, Antarctic Peninsula: responses to climate change. Quaternary Sciences (in Chinese), 34(3): 590–599, doi: 10.3969/j.issn.1001-7410.2014.03.13

Nie Senyan, Xiao Wenshen, Wang Rujian. 2015. Palaeoclimatic changes of the Bransfield Strait, Antarctic Peninsula since 6 kaBP, and the tele-connection with ENSO. Marine Geology & Quaternary Geology (in Chinese), 35(3): 157–166, doi: 10.3724/SP.J.1140.2015.03157

Nie Senyan, Xiao Wenshen, Wang Rujian. 2022. Mid-Late Holocene climate variabilities in the Bransfield Strait, Antarctic Peninsula driven by insolation and ENSO activities. Palaeogeography, Palaeoclimatology, Palaeoecology, 601: 111140, doi: 10.1016/j.palaeo.2022.111140

O'Brien P E, De Santis L, Harris P T, et al. 1999. Ice shelf grounding zone features of western Prydz Bay, Antarctica: sedimentary processes from seismic and sidescan images.

Antarctic Science, 11(1): 78–91, doi: 10.1017/S0954102099000115

Orsi A H, Johnson G C, Bullister J L. 1999. Circulation, mixing, and production of Antarctic Bottom Water. Progress in Oceanography, 43(1): 55–109, doi: 10.1016/S0079-6611(99)00004-X

Orsi A H, Whitworth III T. 2005. Southern Ocean. In: Sparrow M, Chapman P, Gould J, eds. Hydrographic Atlas of the World Ocean Circulation Experiment. Southampton: International WOCE Project Office

Orsi A H, Whitworth III T, Nowlin Jr W D. 1995. On the meridional extent and fronts of the Antarctic Circumpolar Current. Deep-Sea Research Part Ⅰ: Oceanographic Research Papers, 42(5): 641–673, doi: 10.1016/0967-0637(95)00021-W

Passchier S. 2011. Linkages between East Antarctic Ice Sheet extent and Southern Ocean temperatures based on a Pliocene high-resolution record of ice-rafted debris off Prydz Bay, East Antarctica. Paleoceanography, 26(4): PA4204, doi: 10.1029/2010PA002061

Patterson M O, McKay R, Naish T, et al. 2014. Orbital forcing of the East Antarctic ice sheet during the Pliocene and Early Pleistocene. Nature Geoscience, 7(11): 841–847, doi: 10.1038/ngeo2273

Pattyn F, Ritz C, Hanna E, et al. 2018. The Greenland and Antarctic ice sheets under 1.5℃ global warming. Nature Climate Change, 8(12): 1053–1061, doi: 10.1038/s41558-018-0305-8

Pollard D, DeConto R M. 2009. Modelling West Antarctic ice sheet growth and collapse through the past five million years. Nature, 458(7236): 329–332, doi: 10.1038/nature07809

Pondaven P, Ragueneau O, Tréguer P, et al. 2000. Resolving the 'opal paradox' in the Southern Ocean. Nature, 405(6783): 168–172, doi: 10.1038/35012046

Presti M, Barbara L, Denis D, et al. 2011. Sediment delivery and depositional patterns off Adélie Land (East Antarctica) in relation to late Quaternary climatic cycles. Marine Geology, 284(1–4): 96–113, doi: 10.1016/j.margeo.2011.03.012

Prins M A, Bouwer L M, Beets C J, et al. 2002. Ocean circulation and iceberg discharge in the glacial North Atlantic: Inferences from unmixing of sediment size distributions. Geology, 30(6): 555–558, doi: 10.1130/0091-7613(2002)030<0555:OCAIDI>2.0.CO;2

Prothro L O, Majewski W, Yokoyama Y, et al. 2020. Timing and pathways of East Antarctic Ice Sheet retreat. Quaternary Science Reviews, 230: 106166, doi: 10.1016/j.quascirev.2020.106166

Prothro L O, Simkins L M, Majewski W, et al. 2018. Glacial retreat patterns and processes determined from integrated sedimentology and geomorphology records. Marine Geology, 395: 104–119, doi: 10.1016/j.margeo.2017.09.012

Pugh R S, McCave I N, Hillenbrand C D, et al. 2009. Circum-Antarctic age modelling of Quaternary marine cores under the Antarctic Circumpolar Current: ice-core dust–magnetic correlation. Earth and Planetary Science Letters, 284(1–2): 113–123, doi: 10.1016/j.epsl.2009.04.016

Ren Aijun. 1993. The comparison between southern Andes and Antarctic Peninsula: a review, new progress and prospect. East China Geology, 14(4): 60–67

Röthlisberger R, Crosta X, Abram N J, et al. 2010. Potential and limitations of marine and ice core sea ice proxies: an example from the Indian Ocean sector. Quaternary Science Reviews, 29(1–2): 296–302, doi: 10.1016/j.quascirev.2009.10.005

Sayles F L, Martin W R, Chase Z, et al. 2001. Benthic remineralization and burial of biogenic SiO_2, $CaCO_3$, organic carbon, and detrital material in the Southern Ocean along a transect at 170° west. Deep-Sea Research Part Ⅱ: Topical Studies in Oceanography, 48(19–20): 4323–4383, doi: 10.1016/S0967-0645(01)00091-1

Schlitzer R. 2009. Ocean data view. http://odv.awi.de/ [2024-07-01]

Sigman D M, Hain M P, Haug G H. 2010. The polar ocean and glacial cycles in atmospheric CO_2 concentration. Nature, 466(7302): 47–55, doi: 10.1038/nature09149

Sikes E L, Umling N E, Allen K A, et al. 2023. Southern Ocean glacial conditions and their influence on deglacial events. Nature Reviews Earth & Environment, 4(7): 454–470, doi: 10.1038/s43017-023-00436-7

Song Qianwei, Qin Bingbin, Tang Zheng, et al. 2022. Calcification of planktonic foraminifer *Neogloboquadrina pachyderma* (sinistral) controlled by seawater temperature rather than ocean acidification in the Antarctic Zone of modern Southern Ocean. Science China: Earth Sciences (in Chinese), 65(9): 1824–1836, doi: 10.1007/s11430-021-9924-7

Starr A, Hall I R, Barker S, et al. 2021. Antarctic icebergs reorganize ocean circulation during Pleistocene glacials. Nature, 589(7841): 236–241, doi: 10.1038/s41586-020-03094-7

Tang Zheng, Li Tiegang, Xiong Zhifang, et al. 2022. Covariation of deep Antarctic-Pacific oxygenation and atmospheric CO_2 during the last 770 kyr. Lithosphere, 2022(S9): 1835176, doi: 10.2113/2022/1835176

Tang Zheng, Shi Xuefa, Zhang Xu, et al. 2016. Deglacial biogenic opal peaks revealing enhanced Southern Ocean upwelling during the last 513 ka. Quaternary International, 425: 445–452, doi: 10.1016/j.quaint.2016.09.020

Tigchelaar M, Timmermann A, Pollard D, et al. 2018. Local insolation changes enhance Antarctic interglacials: insights from an 800, 000-year ice sheet simulation with transient climate forcing. Earth and Planetary Science Letters, 495: 69–78, doi: 10.1016/j.epsl.2018.05.004

Toggweiler J R, Russell J L, Carson S R. 2006. Midlatitude westerlies, atmospheric CO_2, and climate change during the ice ages. Paleoceanography, 21(2): PA2005, doi: 10.1029/2005PA001154

Wagner M, Hendy I L. 2017. Trace metal evidence for a poorly ventilated glacial Southern Ocean. Quaternary Science Reviews, 170: 109–120, doi: 10.1016/j.quascirev.2017.06.

014

Wang Baishun, Chen Zhihua, Wang Ximeng, et al. 2014. The sedimentary hydrodynamic environment of the south Powell Basin, Antarctic Peninsula since MIS3. Chinese Journal of Polar Research (in Chinese), 26(1): 120–127, doi: 10.13679/j.jdyj.2014.1.120

Wang Tong, Hu Yihao, Jia Qi, et al. 2023a. Productivity evolution in the Antarctic Weddell Sea and its paleoceanographic implication since MIS 5. Marine Geology & Quaternary Geology (in Chinese), 43(3): 144–156, doi: 10.16562/j.cnki.0256-1492.2022112302

Wang Jiakai, Li Tiegang, Tang Zheng, et al. 2022a. Relating the composition of continental margin surface sediments from the Ross Sea to the Amundsen Sea, West Antarctica, to modern environmental conditions. Advances in Polar Science, 33(1): 55–70, doi: 10.13679/j.advps.2021.0005

Wang Jiakai, Li Tiegang, Xiong Zhifang, et al. 2018. Sedimentary gochemical characteristics of the Redox-sensitive elements in Ross Sea, Antarctica: implications for paleoceanography. Marine Geology & Quaternary Geology (in Chinese), 38(5): 112–121, doi: 10.16562/j.cnki.0256-1492.2018.05.011

Wang Rujian, Polyak L, Xiao Wenshen, et al. 2023b. Middle to Late Quaternary changes in ice rafting and deep current transport on the Alpha Ridge, central Arctic Ocean and their responses to climatic cyclicities. Global and Planetary Change, 220: 104019, doi: 10.1016/j.gloplacha.2022.104019

Wang Jiakai, Tang Zheng, Wilson D J, et al. 2022b. Ocean-forced instability of the West Antarctic Ice Sheet since the Mid-Pleistocene. Geochemistry, Geophysics, Geosystems, 23(9): e2022GC010470, doi: 10.1029/2022GC010470

Wang Pinxian, Tian Jun, Cheng Xinrong, et al. 2003. Carbon reservoir changes preceded major ice-sheet expansion at the mid-Brunhes event. Geology, 31(3): 239–242, doi: 10.1130/0091-7613(2003)031<0239:CRCPMI>2.0.CO;2

Wang Rujian, Xiao Wenshen, März C, et al. 2013. Late Quaternary paleoenvironmental changes revealed by multi-proxy records from the Chukchi Abyssal Plain, western Arctic Ocean. Global and Planetary Change, 108: 100–118, doi: 10.1016/j.gloplacha.2013.05.017

Weber M E, Kuhn G, Sprenk D, et al. 2012. Dust transport from Patagonia to Antarctica —a new stratigraphic approach from the Scotia Sea and its implications for the last glacial cycle. Quaternary Science Reviews, 36: 177–188, doi: 10.1016/j.quascirev.2012.01.016

Williams G D, Bindoff N L, Marsland S J, et al. 2008. Formation and export of dense shelf water from the Adélie Depression, East Antarctica. Journal of Geophysical Research: Oceans, 113(C4): C04039, doi: 10.1029/2007JC004346

Wilson D J, Bertram R A, Needham E F, et al. 2018. Ice loss from the East Antarctic Ice Sheet during late Pleistocene interglacials. Nature, 561(7723): 383–386, doi: 10.1038/s41586-018-0501-8

Wu Li, Li Longwei, Wang Rujian, et al. 2024. Grain-size, coarse fraction lithology and clay mineral compositions of surface sediments from Ross Sea, Antarctica: implications for their provenance and delivery mode. Frontiers in Marine Science, 10: 1324391, doi: 10.3389/fmars.2023.1324391

Wu Shiguo, Lu Jun. 1998. Paleoclimatic evolution recorded in sediments of the Prydz Bay, Antarctica in 15 000 years. Haiyang Xuebao (in Chinese), 20(1): 65–73

Wu Li, Wang Rujian, Krijgsman W, et al. 2019. Deciphering color reflectance data of a 520 kyr sediment core from the Southern Ocean: method application and paleoenvironmental implications. Geochemistry, Geophysics, Geosystems, 20(6): 2808–2826, doi: 10.1029/2019GC008212

Wu Li, Wang Rujian, Xiao Wenshen, et al. 2017. Productivity-climate coupling recorded in Pleistocene sediments off Prydz Bay (East Antarctica). Palaeogeography, Palaeoclimatology, Palaeoecology, 485: 260–270, doi: 10.1016/j.palaeo.2017.06.018

Wu Li, Wang Rujian, Xiao Wenshen, et al. 2018. Late Quaternary deep stratification-climate coupling in the Southern Ocean: implications for changes in abyssal carbon storage. Geochemistry, Geophysics, Geosystems, 19(2): 379–395, doi: 10.1002/2017GC007250

Wu Li, Wilson D J, Wang Rujian, et al. 2020. Evaluating Zr/Rb ratio from XRF scanning as an indicator of grain-size variations of glaciomarine sediments in the Southern Ocean. Geochemistry, Geophysics, Geosystems, 21(11): e2020GC009350, doi: 10.1029/2020GC009350

Wu Li, Wilson D J, Wang Rujian, et al. 2021. Late Quaternary dynamics of the Lambert Glacier-Amery Ice Shelf system, East Antarctica. Quaternary Science Reviews, 252: 106738, doi: 10.1016/j.quascirev.2020.106738

Xiao Wenshen, Frederichs T, Gersonde R, et al. 2016. Constraining the dating of late Quaternary marine sediment records from the Scotia Sea (Southern Ocean). Quaternary Geochronology, 31: 97–118, doi: 10.1016/j.quageo.2015.11.003

Xiu Chun, Chen Xinxi, Zhou Mengjia, et al. 2017. REE geochemical characteristics of core R11 in the Ross Sea, Antarctic. Marine Geology Frontiers (in Chinese), 33(5): 1–8, doi: 10.16028/j.1009-2722.2017.05001

Yabuki T, Suga T, Hanawa K, et al. 2006. Possible source of the Antarctic bottom water in the Prydz Bay region. Journal of Oceanography, 62(5): 649–655, doi: 10.1007/s10872-006-0083-1

Yan Bin, Xie Jingqian, Wu Li, et al. 2023. Coupling between iceberg rafted debris events and bottom current activities in the northwestern Weddell Sea during the last glacial period. Chinese Journal of Polar Research (in Chinese), 35(4): 542–555, doi: 10.13679/j.jdyj.20220437

Yang Chunli, Chen Zhihua, Xiao Wenshen, et al. 2021. Paleoproductivity and its environmental constraints in the Scotia Sea, Antarctica since 34 ka BP. Haiyang Xuebao (in Chinese), 43(3): 116–125, doi: 10.12284/hyxb2021051

Yin Qiuzhen, Berger A. 2010. Insolation and CO_2 contribution to the interglacial climate before and after the Mid-Brun-

hes Event. Nature Geoscience, 3(4): 243–246, doi: 10.1038/ngeo771

Zhang Yongcong, Hu Liangming, Sun Xi, et al. 2023a. Rare earth element and Sr-Nd isotopic characteristics of the sediments in Antarctic Cosmonaut Sea and their provenance significances since the late Middle-Holocene. Haiyang Xuebao (in Chinese), 45(5): 14–26, doi: 10.12284/hyxb2023076

Zhang Qiang, Roberts A P, Ge Shulan, et al. 2022. Interpretation of anhysteretic remanent magnetization carriers in magnetofossil-rich marine sediments. Journal of Geophysical Research: Solid Earth, 127(11): e2022JB024432, doi: 10.1029/2022JB024432

Zhang Jingyuan, Xiao Wenshen, Wang Rujian, et al. 2023b. Changes in productivity and ice-rafting input in the Amundsen Sea during the Late Pleistocene: Implications on the evolution of surface-ocean environment and the West Antarctic Ice Sheet. Marine Geology & Quaternary Geology (in Chinese), 43(2): 136–144, doi: 10.16562/j.cnki.0256-1492.2023020802

Zhao Renjie, Chen Zhihua, Liu Helin, et al. 2017. Sedimentary record and paleoceanographic implications of the core on the continental shelf off the Ross Sea since 15 ka. Haiyang Xuebao (in Chinese), 39(5): 78–88